HHS Public Access

Author manuscript

J Immunol. Author manuscript; available in PMC 2016 June 06.

Published in final edited form as:

J Immunol. 2008 December 15; 181(12): 8534–8543.

A Role for Connexin43 in Macrophage Phagocytosis and Host Survival after Bacterial Peritoneal Infection[1]

Rahul J. Anand[#*,†], **Shipan Dai**[#*,†], **Steven C. Gribar**[*,†], **Ward Richardson**[*,†], **Jeff W. Kohler**[*,†], **Rosemary A. Hoffman**[†], **Maria F. Branca**[*,†], **Jun Li**[*,†], **Xiao-Hua Shi**[*,†], **Chhinder P. Sodhi**[*,†], and **David J. Hackam**[3,*,†]

[*]Division of Pediatric Surgery, Children's Hospital of Pittsburgh, and University of Pittsburgh School of Medicine, Pittsburgh, PA 15213

[†]Department of Surgery, University of Pittsburgh School of Medicine, Pittsburgh, PA, 15213

[#] These authors contributed equally to this work.

Abstract

The pathways that lead to the internalization of pathogens via phagocytosis remain incompletely understood. We now demonstrate a previously unrecognized role for the gap junction protein connexin43 (Cx43) in the regulation of phagocytosis by macrophages and in the host response to bacterial infection of the peritoneal cavity. Primary and cultured macrophages were found to express Cx43, which localized to the phagosome upon the internalization of IgG-opsonized particles. The inhibition of Cx43 using small interfering RNA or by obtaining macrophages from Cx43 heterozygous or knockout mice resulted in significantly impaired phagocytosis, while transfection of Cx43 into Fc-receptor expressing HeLa cells, which do not express endogenous Cx43, conferred the ability of these cells to undergo phagocytosis. Infection of macrophages with adenoviruses expressing wild-type Cx43 restored phagocytic ability in macrophages from Cx43 heterozygous or deficient mice, while infection with viruses that expressed mutant Cx43 had no effect. In understanding the mechanisms involved, Cx43 was required for RhoA-dependent actin cup formation under adherent particles, and transfection with constitutively active RhoA restored a phagocytic phenotype after Cx43 inactivation. Remarkably, mortality was significantly increased in a mouse model of bacterial peritonitis after Cx43 inhibition and in Cx43 heterozygous mice compared with untreated and wild-type counterparts. These findings reveal a novel role for Cx43 in the regulation of phagocytosis and rearrangement of the F-actin cytoskeleton, and they implicate Cx43 in the regulation of the host response to microbial infection.

[1]This work was supported by National Institutes of Health Grant RO1 GM078238-01 (to D.J.H.), the Resident Research Award from the Surgical Infection Society (to R.J.A.), and from the American College of Surgeons (to S.C.G.), as well as a Loan Repayment Award from the National Institutes of Health (to S.C.G.).

[3] Address correspondence and reprint requests to Dr. David J. Hackam, Children's Hospital of Pittsburgh, 3705 Fifth Avenue, 4A485 DeSoto Wing, Pittsburgh, PA 15213. ; Email: david.hackam@chp.edu

The costs of publication of this article were defrayed in part by the payment of page charges. This article must therefore be hereby marked *advertisement* in accordance with 18 U.S.C. Section 1734 solely to indicate this fact.

Disclosures

The authors have no financial conflicts of interest.

Phagocytosis is the first line of defense against invading pathogens and requires a dramatic rearrangement of the actin cytoskeleton to internalize invading microbes into the membrane-bound phagosome ([1–3]). The mechanisms that regulate the reorganization of the actin cytoskeleton underneath particles that are adherent to the surface of macrophages remain incompletely understood. To investigate the early events that lead to particle internalization via phagocytosis, we now focus on the role of the integral membrane protein connexin43 (Cx43).[4] Cx43 is an important component of gap junctions, intercellular channels that allow the passage of molecules <1000 Da between adjacent cells (for a recent review, please see Ref. [4]). Gap junctions are formed at opposing sides of adjacent plasma membranes through the interaction of paired connexon monomers, also known as hemichannels ([5]). Recent evidence has indicated that hemichannels are present within cells that do not form gap junctions, and also that connexins may exert important functions that do not involve intercellular channels ([6]). Evidence from a variety of sources suggests that such functions could potentially play a role in the regulation of phagocytosis by macrophages, which are not interconnected in most cases, through several potential mechanisms. For instance, hemichannel activity has been shown to alter calcium stores in cells, long known to be important in the regulation of phagocytosis ([7]), through the activation of purinergic P2 receptors by ATP ([8]). Cx43 has also been shown to interact with a variety of cytoskeletal proteins ([9–11]), suggesting the possibility that Cx43 could modify the actin cytokeleton in the early events leading to phagocytosis. As a further rationale for the study of connexins in phagocytosis, connexins have been shown to be present in immune cells, including macrophages, although their role in these cells remains largely unknown ([12–14]). A role for Cx43 in the regulation of phagocytosis would represent an exciting departure from current thinking in this area, for it would demonstrate a previously unrecognized role for this membrane protein in the modulation of an essential component of the host immune response. We therefore sought to test the hypothesis that Cx43 would play a role in the initiation or regulation of phagocytosis through effects on the actin cytoskeleton.

In support of this hypothesis, we now demonstrate the surprising findings that Cx43 plays an important role in the regulation of phagocytosis, that Cx43 appears to act by interaction with the RhoA signaling pathway and the modulation of the actin cytoskeleton, and that the regulation of phagocytosis by Cx43 plays a role in the host response to bacterial infection.

Materials and Methods

Cell culture, harvest, treatment, and reagents

HeLa cells and the murine macrophage cell lines J774 and RAW264.7 were obtained from the American Type Culture Collection (ATCC) and maintained in DMEM supplemented with 10% FBS, 1% glutamine, 100 U/ml penicillin, and 100 μg/ml streptomycin at 37°C in a 5% CO_2 atmosphere. Abs were obtained from the following sources: Cx43 (Chemicon International), lysosomal-associated membrane protein 2 (LAMP-2; Zymed Laboratories), p38 (Cell Signaling Technology), RhoA (Cytoskeleton), and CD45 (Abcam). Sheep RBC

[4]Abbreviations used in this paper: Cx43, connexin43; DIC, differential interference contrast; dn, dominant negative; LAMP-2, lysosomal-associated membrane protein 2; LPA, lysophasphatidic acid; siRNA, small interfering RNA; SRBC, sheep RBC; wt, wild type.

were from Fitzgerald Industries International. Dynabeads (nonconjugated, noncross-linked, nondyed, 3 μm) were from Dynal Biotech. All other reagents were from Sigma-Aldrich.

Genotyping of mice was confirmed by PCR using tail tip genomic DNA, which was prepared by the proteinase K digestion method ([16]). The following primers were used: CCCCACTCTCACCTATGTCTCC, ACTTT TGCCGCCTAGCTATCCC, CTTGGGTGGAGAGGCTATTC, AGGT GAGATGACAGGAGATC. For PCR analyses, genomic DNA was used as a template in a reaction, where wild-type and mutant alleles are detected in a reaction simultaneously. PCR reactions were performed in 25 μl reaction volume containing forward and reverse primers, *Taq* polymerase, and PCR buffer (Invitrogen). The PCR conditions were 95°C for 5 min hold, 12 cycles of 95°C for 30 s, 64°C for 30 s, and 72°C for 1 min, and 25 cycles of 95°C for 30 s, 55°C for 30 s, and 72°C for 1 min in MyCycler PCR system (Bio-Rad). This will generate a 519-bp amplicon for wild-type, a 519-bp amplicon and a 280-bp amplicon for heterozygote, and a 280-bp amplicon for homozygote. The PCR-amplified products were separated through 2% agarose in 1× TAE (40 mM Tris acetate, 1 mM EDTA (pH 8.2)) gels and photographed using an Alpha Innotech Imager 2000.

Peritoneal macrophages were obtained from male C57BL/6 mice and male connexin heterozygote mice (The Jackson Laboratory) by peritoneal lavage. Cells were harvested when animals were at 4–6 wk of age; all animal experiments were performed in accordance with the Children's Hospital of Pittsburgh Animal Care and Use Committee guidelines (protocol 08-05). Where indicated, animals were treated with i.p. injections of oleamide (12.5, 25, or 50 mg/kg, once daily) for 3 days. Animals were sacrificed and macrophages were then harvested as follows: after cleansing the skin with 70% ethanol, an incision was made in the lower abdomen through the skin, leaving the peritoneum intact. Animals were then injected with 10 ml ice-cold PBS followed by gentle massage to allow for the distribution of the lavage fluid throughout the peritoneal cavity. The PBS lavage fluid was then removed using a 10-ml syringe attached to a 21-guage needle, and cells were washed three times in DMEM + 10% FBS. Macrophages were identified by adherence to glass coverslips (1 h, 37°C) and morphology characteristics under light microscopy. In all experiments, there were at least eight animals per group and each experiment was performed at least four times.

Isolation of embryonic liver macrophages

To study macrophages from Cx43-null mice, which die shortly after birth, macrophages were harvested from embryonic liver in an adaptation of the technique of Morris and colleagues ([17]). Pregnant females were sacrificed at embryonic days 16–18 from the strains $Cx43^{+/+}$, $Cx43^{+/-}$, and $Cx43^{-/-}$, which were mated from Cx43 heterozygotes (strain B6;129S-Gja1^{tm1Kdr}/J, The Jackson Laboratory). Embryos were removed and washed in ice-cold PBS. Tails were clipped and snap-frozen for genotyping. Livers were dissected under a Nikon SMZ1000 dissecting microscope, washed with PBS, minced into small pieces, and digested with 0.05% collagenase and 0.02% DNase in DMEM for 60 min at 37°C with gentle pipetting to dissociate tissue. Cells were taken from the supernatant after allowing the suspension to settle for 1 min, washed in DMEM three times, plated on glass coverslips, and

incubated for 4–6 h at 37°C, 5% CO_2. Unattached cells were washed off with ice-cold PBS and the remaining cells were allowed to attach for a subsequent 6 h before use. This technique yielded a population of cells that was >95% positive for macrophages as previously described ([17]), and as demonstrated by the macrophage marker CD45. Phagocytosis experiments using these cells were performed in a blinded fashion (i.e., without the knowledge of the genotype results of the individual mice studied) on at least 12 mice per experiment.

SDS-PAGE and immunofluorescence

For detection of Cx43 or CD45 expression, cells were lysed and protein concentration was measured using the bicinchoninic acid assay (Sigma-Aldrich). Lysates were then subjected to SDS-PAGE as described ([18]) and immunoblotted using Abs against Cx43 (1/1000). In parallel, cells were plated on glass coverslips, washed three times in ice-cold PBS, fixed in 4% paraformaldehyde, and immunostained using Abs against Cx43 and visualized using confocal microscopy (Olympus FluoView 1000) as described ([19]). For studies to detect the presence of Cx43 on the phagosomal membrane, J774 macrophages were allowed to internalize Dynabeads on coverslips in 12-well dishes (90 μl/well) for 30 min at 37°C, washed in ice-cold PBS, and then fixed in 4% paraformaldehyde and evaluated by immunofluorescence microscopy as described ([19]). Actin cup formation was quantified using MetaMorph 7 software (Molecular Devices), during which an actin cup was defined as the local enrichment of F-actin immediately subjacent to an adherent particle. Where indicated, actin was detected by staining cells with rhodamine-phalloidin (Molecular Probes/Invitrogen).

Phagosomal fractions were isolated according to the method of Desjardins et al. ([1]) and modified by Hackam and colleagues ([20]). Briefly, cells were plated on 10-cm petri dishes in 5 ml of DMEM with 10% FBS until they reached 80% confluence. Latex beads (0.8-μm-diameter blue dyed, Sigma-Aldrich) were added to the cells (90 μl beads in 10 cc media) for 2 h at 37°C to allow phagocytosis to occur. Cells were then washed three times in ice-cold PBS (10 min each, with continuous shaking) and homogenized in a Dounce homogenizer until 90% of cells were broken, as assessed by light microscopy. The homogenate was next subjected to centrifugation at 350 × *g* for 5 min. The resulting supernatant was mixed with 60% sucrose and 3 mM of imidazole (pH 7.4) and applied to the bottom of a discontinuous sucrose gradient composed of the following 2-ml steps: 10%, 25%, 35%, and 40% sucrose-imidazole. The gradient was subjected to centrifugation at 100,000 × *g* for 60 min, and the phagosomal fraction was collected from the 10–25% interface. This was added to 15 ml of PBS and centrifuged at 40,000 × *g* for 15 min. The phagosomal pellet was solubilized for immunoblotting following SDS-PAGE, or was evaluated for purity by transmission electron microscopy. We have demonstrated that this preparation yields a fraction that is >95% pure phagosomal material, without contaminating organelles or cells ([20]).

Measurement of phagocytosis

To accurately quantify the rate and extent of phagocytosis, it was critical to reliably distinguish particles that were internalized from those that were merely adherent to the macrophage surface. To do so, three separate approaches were utilized: an in vitro sheep

RBC assay, an in vitro bead (confocal-based) assay, and an in vivo-labeled bacteria assay as follows:

Sheep RBC assay—The following experimental protocol was adapted from that of Grinstein and colleagues ([2]). In brief, sheep RBC (SRBCs, Fitzgerald Industries International) were opsonized by incubating with anti-RBC IgG (Sigma-Aldrich, 1/10 dilution from stock, 20 min, 37°C) and were then added to J774 cells, murine peritoneal macrophages, or murine embryonic hepatic macrophages that had been plated overnight on glass coverslips at 60% confluence (SRBC/macrophage ratio 10:1, 30 min incubation at 37°C). Noninternalized SRBCs were then removed by hypotonic lysis with ice-cold water for 30 s. After washing with ice-cold PBS, cells were fixed in 4% paraformaldehyde for 1 h. Phagocytosis was then assessed using a Nikon Eclipse TS100 microscope under phase contrast optics, under which only internalized particles appear. The number of macrophages that had internalized at least one SRBC was then measured.

Bead internalization assay—Macrophages were incubated with Dynabeads under the above conditions in the presence of 10% FCS. After allowing phagocytosis to occur (5, 15, 30, 60, or 120 min, 37°C), noninternalized particles were removed by copious washes with PBS. Internalized particles were distinguished from extracellular particles using an Olympus Fluo-View 1000 confocal microscope under differential interference contrast (DIC) filters, during which slices were obtained throughout the plane of the cell. A three-dimensional reconstruction was developed for each field, with planes obtained from the top of the cell to the coverslip, which reliably identified noninternalized particles. At the indicated time point, cells were fixed, permeabilized, and stained with Abs to Cx43 and examined by confocal microscopy.

To assess whether bead internalization was FcR-mediated, RAW264.7 macrophages or J774 cells were washed in serum-free conditions, then treated with anti-FcR Ab (mouse monoclonal hybridoma supernatant 2.4G2 from ATCC) or nonspecific anti-mouse IgG (Sigma-Aldrich) for 1 h, and allowed to undergo phagocytosis of either Dynabeads or latex particles for 1 h at 37°C. The rate of phagocytosis was then determined as described below.

To assess particle binding, RAW264.7 macrophages were incubated with Dynabeads in the presence of serum and placed at 4°C for 1 h, then washed with ice-cold PBS, and the number of bead-associated particles was assessed by light microscopy. In parallel, RAW264.7 macrophages were treated with cytochalasin D (100 μM; 1 h, Sigma-Aldrich) ([19, 20]), treated with Dynabeads in the presence of serum for 1 h at 37°C, then washed with copious amounts of ice-cold PBS and assessed for the number of bead-associated particles by light microscopy. Where indicated, RAW264.7 macrophages were first treated with small interfering RNA (siRNA) to Cx43 or scrambled (control) siRNA as described below.

In vivo phagocytosis assay—C57BL/6 mice (n = 5 mice/group) were treated with either vehicle (0.5% ethanol in PBS) or oleamide (5 mg/kg) daily for 3 days. On the third day of treatment, mice were injected i.p. with *Escherichia coli* (8×10^8 CFU/mouse, DH5a; Invitrogen) labeled with Oregon Green (Invitrogen, 1 mg/ml in PBS for 1 h at 37°C) as per the manufacturer's instructions. After allowing 2 h for internalization of labeled bacteria,

peritoneal macrophages were harvested as described above by lavage. In parallel experiments, Oregon Green-labeled bacteria were injected into the peritoneal cavities of either wild-type or $Cx43^{+/-}$ mice, and macrophages were harvested 2 h later. Harvested macrophages were plated on glass coverslips, and after allowing 20 min for adherence, cells were washed with copious amounts of ice-cold PBS to remove noninternalized bacteria. Macrophages were then fixed using 4% paraformaldehyde, and examined using confocal microscopy (Olympus FluoView 1000) under DIC and FITC filter sets, which could reliably detect internalized fluorescent particles. Where indicated, macrophages were subjected to siRNA transfection (see below), treatment with IFN-γ (100 U/ml) and LPS (10 ng/ml), (12 h), with the gap junction protein inhibitor oleamide (50 μM, 1 h), with the Rho activator lysophasphatidic acid (LPA, 10 μM, 30 min), or with the Rho inhibitor Y27632 (10 μM, 1 h).

Activation and inhibition of Cx43 using siRNA

To inhibit the expression of Cx43 in RAW264.7 macrophages, cells were plated onto 6-well culture dishes (500,000 cells/well, Sigma-Aldrich). After allowing 24 h for adhesion, the medium was changed and cells were treated with 20 μl of pooled Cx43 siRNA (5 nM, Ambion) and 10 μl Lipofectamine 2000 (Invitrogen) in OptiMEM media (Invitrogen). Six hours later, wells were repleted with DMEM containing 10% FBS. After 24 h, cells were re-treated with the original concentration of siRNA. Five days after the initial plating, cells were harvested, lysed, and assessed by SDS-PAGE for the expression of Cx43 and actin as described above, or evaluated for the ability to undergo phagocytosis. In all experiments, a nontargeting siRNA engineered against no specific gene (5 nM) was included in all as a negative control. RhoA activity was “restored” using a constitutively active form of RhoA (V-14 RhoA, a generous gift from Dr. Michael S. Kolodney, University of California at Los Angeles School of Medicine) using Lipofectamine 2000 as a carrier molecule according to the manufacturer's protocol.

HeLa cells were transfected with the following cDNA constructs alone or in combination: GFP-Cx43 (a generous gift of Dr. M Falk, Lehigh University, Bethlehem, PA), FcRIIa (a generous gift from Dr. Allan D. Schreiber, University of Pennsylvania School of Medicine, Philadelphia, PA), and enhanced GFP (Clontech) using Lipofectamine 2000 as a carrier according to the manufacturer's instructions.

Generation of Cx43 adenoviruses

Adenoviruses expressing wild-type (wt) or dominant-negative (dn) (L90V) Cx43 with the C-terminal fused to GFP were constructed using the Adeno-X Expression Systems 2 from Clontech according to the manufacturer's protocol. Briefly, cDNAs coding for GFP, wtCx43, and dnCx43 (L90V) (generous gifts of Dr. Charles Murry, University of Washington, Seattle, WA; Dr. Dale Laird, University of Western Ontario, London, Ontario, Canada) ([21], [22]) were cloned into pDNR-CMV and integrated into Adeno-X acceptor vectors by using Cre-*loxP* site-specific recombination. The resulting plasmids were linearized with *Pac*I digestion and transfected into the adenovirus packaging cell line HEK293. Adenoviruses were further amplified and titered in HEK293 cells. In all experiments, macrophages were then infected with viruses at a multiplicity of infection of ~20. At this ratio, all cells were found to express

GFP-wtCx43 or GFP-dnCx43 as determined under fluorescent microscopy using an excitation wavelength of 390 nm and emission wavelength of 505 nm. The expression and distribution of GFP-Cx43 was similar to that of endogenous Cx43 in macrophages, as confirmed by confocal microscopy (not shown).

Determination of RhoA-GTPase activation

RhoA-GTPase activity was quantified using an ELISA-based detection assay (Cytoskeleton). Briefly, RAW264.7 macrophages were treated with either Cx43-siRNA or control siRNA as above, and after indicated treatment were subjected to hypotonic lysis at 4°C. The relative expression of activated RhoA-GTP to inactive RhoA-GDP was determined spectrofluorometrically based on the increased avidity of RhoA-GTP for the effector protein rhotekin, as we and others have previously described ([23], [24]). Positive controls included samples enriched with GTP-γS to maximize RhoA activation.

Induction of experimental bacterial peritonitis

Mice were genotyped and matched to age (4–5 wk) and weight, then injected with 1×10^5 CFU/g of *E. coli* (strain DH5a) daily for 3 days. Where indicated, mice were also injected daily for 3 days with either oleamide (12.5, 25, or 50 mg/kg) or saline. The number of animals alive on each day was measured, and the mortality rate at the end of the 3-day period was determined. At least 10 mice in each group were studied.

Statistics

Phagocytosis was quantified by dividing the number of cells per high-power field that had phagocytosed at least one particle by the total number of phagocytic cells per high-power field. For quantification of phagocytosis, at least 10 fields were examined and enumerated per experimental condition. In experiments performed on embryonic macrophages, the rate of phagocytosis of GFP-wtCx43 and GFP-dnCX43 was normalized to the rate of GFP-infected macrophages for the indicated treatment group. All experiments were repeated at least five times. Comparisons were made by Student's *t* test and ANOVA where appropriate. Kaplan-Meier survival curves were calculated using the online Bioinformatics software package of the Walter and Eliza Hall Institute of Medical Research, University of Melbourne.

Results

Cx43 is expressed on the phagosome in macrophages

To test the hypothesis that Cx43 may participate in phagocytosis, we first evaluated the expression of Cx43 in macrophages and on phagosomes. As shown in Fig. 1*A*, Cx43 expression could be detected in J774 and RAW264.7 macrophage cell lines, as well as in elicited murine peritoneal macrophages from $Cx43^{+/+}$ mice. There was a decreased yet detectable band obtained in macrophages from $Cx43^{+/-}$ mice. To investigate whether Cx43 was delivered to the nascent phagosome, as would be predicted if it has a role in phagocytosis, we performed immunoconfocal microscopy of RAW264.7 macrophages that had been allowed to internalize Dynabeads in the presence of serum for varying time points as described in *Materials and Methods*. As shown in Fig. 1*B*, Cx43 (green staining) was

detectable immediately underneath particles that were adherent to the cell surface (seen in the DIC images), and it became associated with the phagosomal membrane at the earliest time points after internalization (see arrows at the 15-min time point). Importantly, in cells that were allowed to undergo phagocytosis for longer periods, Cx43 was detected on the phagosomal membrane at all time points (see arrows in Fig. 1*B*). It is noteworthy that the number of internalized particles increased over time, and Cx43 was detected around each particle. To confirm these findings, a biochemical approach was taken. Specifically, we performed subcellular fractionation and phagosomal isolation of J774 cells that had been allowed to internalize latex particles for 2 h, as described in *Materials and Methods*. The purity of the membrane preparation has been confirmed earlier ([2], [25]), and it was found to express the lysosomal marker LAMP-2 and to be devoid of the cytoplasmic protein p38 (Fig. 1*C*). Importantly, purified phagosomes were found to express Cx43 (Fig. 1*C*), consistent with the confocal findings. Of note, the principal receptor that was found to govern phagocytosis of Dynabeads (Fig. 1*B*) and latex beads (Fig. 1*C*) was determined to be the FcR, as Abs against FcR significantly reduced the extent of phagocytosis of both types of particles that were detected (Fig. 1*D*). Based on these results, we next investigated whether Cx43 participated in phagocytosis.

Cx43 plays a role in phagocytosis by macrophages

As shown in Fig. 2, three lines of evidence support the conclusion that Cx43 participates in macrophage phagocytosis. Treatment of macrophages with the gap junction inhibitor oleamide ([26]) was found to significantly reduce the ability of J774 cells to undergo phagocytosis of IgG-opsonized erythrocytes (Fig. 2*A*, OLM). There was no effect of vehicle control (0.5% ethanol in PBS). There were also no effects of oleamide on cell viability or on the responsiveness of macrophages to release NO in response to activation by LPS (data not shown), excluding effects of oleamide on these cell functions. To further assess these pharmacologic results, a siRNA approach was undertaken to more specifically determine the role of Cx43 in phagocytosis. Compared with untreated cells or cells treated with control siRNA against no known target, treatment of RAW264.7 macrophages with siRNA against Cx43 led to a significant reduction in the expression of Cx43 and also to a striking reduction in the rate of phagocytosis (Fig. 2*B*). Importantly, as shown in Fig. 2*C*, Cx43 did not appear to play a role in the adhesion of particles to macrophages, as the number of Dynabeads that were adherent to the surface of RAW264.7 macrophages that were treated either at 4°C or with the phagocytosis inhibitor cytochalasin D was similar in the presence (open bars) or absence (filled bars) of Cx43. We next assessed the rate of phagocytosis in macrophages obtained from mice with a genetic reduction in the expression of Cx43 ([27]). As shown in Fig. 2*D*, a marked reduction in phagocytic ability was observed by peritoneal macrophages that were harvested from $Cx43^{+/-}$ mice as compared with $Cx43^{+/+}$ mice. Taken together, these findings strongly suggest that Cx43 plays a role in phagocytosis.

Heterologous transfection of cells lacking Cx43 with FcR and Cx43 confers phagocytic ability to HeLa cells

Having shown that the inhibition or relative absence of Cx43 leads to a decrease in phagocytic ability in macrophages, we next sought to further assess the role of Cx43 in phagocytosis by utilizing a knock-in approach. Since all macrophage cell lines that we

assessed were found to express Cx43, we performed these experiments using a heterologous transfection approach in HeLa cells, which lack Cx43, but also lack phagocytic Fc receptors (Fig. 3). Previous authors, including ourselves, have demonstrated that transfection of FcR into non-FcR-expressing cells, including fibroblasts ([28]) and intestinal epithelial cells ([19]), confers the target cell a phagocytic phenotype upon expression of FcR protein. We therefore sought to determine the rate of phagocytosis in Fc-transformed HeLa cells in the absence or presence of cotransfected Cx43. As is shown in Fig. 3, incubation of nontransfected HeLa cells with IgG-opsonized erythrocytes did not result in either significant adhesion or internalization (Fig. 3*A*). Transfection of HeLa cells with the FcIIR phagocytic receptor (along with GFP to identify transfected cells) resulted in the adherence of subsequently added IgG-opsonized erythrocytes, but not to their internalization (Fig. 3, *B* and *C*). Remarkably, cotransfection of HeLa cells with both Cx43 and FcIIR resulted in significant internalization of IgG-opsonized erythrocytes, compared with nontransfected cells, or cells transfected with cDNA alone (Fig. 3, *D*–*F*). The expression of GFP-Cx43 by SDS-PAGE in nontransfected and transfected HeLa cells, as well as in macrophages (positive control), is shown in Fig. 3*G*. Note that GFP-Cx43-transfected HeLa cells demonstrate a band at ~70 kDa, the combined molecular mass of Cx43 and GFP, whereas no bands are detected in nontransfected HeLa cells or GFP-transfected HeLa cells. The location of Cx43 in macrophages, the positive control, at 43 kDa is revealed by the arrow. Taken in aggregate, these knock-in results support the evidence obtained from the deletion studies described above and demonstrate a role for Cx43 in phagocytosis.

Cx43 transfection restores phagocytosis in Cx43-deficient macrophages

We next sought to determine whether we could reverse the inhibition in phagocytosis observed in Cx43-deficient macrophages solely by inducing Cx43 expression. Because Cx43-null mice die shortly after birth ([29]), macrophages were harvested late in gestation (embryonic days 15–18) from the livers of $Cx43^{+/+}$, $Cx43^{+/-}$, and $Cx43^{-/-}$ fetuses. As is shown in Fig. 4*A*, we were able to harvest a relatively pure population of embryonic hepatic macrophages, as shown by the high expression of the macrophage marker CD45. Importantly, embryonic hepatic macrophages obtained from $Cx43^{+/+}$ mice underwent phagocytosis of IgG-opsonized RBCs efficiently. However, the rate of phagocytosis was significantly decreased in those macrophages obtained from $Cx43^{+/-}$ mice (Fig. 4*B*, a finding consistent with the results shown in Fig. 2*C*). The rate of phagocytosis was further decreased in embryonic hepatic macrophages obtained from $Cx43^{-/-}$ mice, consistent with a role for Cx43 in the regulation of phagocytosis (Fig. 4*B*).

Having determined the phagocytic ability of macrophages from wild-type, heterozygous, and Cx43-null mice, we next sought to assess the effects of overexpression of Cx43 on phagocytosis in macrophages from these mice. Infection of embryonic macrophages with adenoviruses that express GFP-Cx43 resulted in a pattern of GFP expression similar to that of endogenous Cx43 in >90% of cells (data not shown). Remarkably, infection of Cx43 in embryonic macrophages obtained from $Cx43^{-/-}$ mice led to a marked increase in the rate of phagocytosis, as compared with $Cx43^{-/-}$ macrophages that were infected with GFP alone (see Fig. 4*C*, compare green bars to yellow bars). Infection with adenoviral GFP-Cx43 also led to an increase in phagocytosis in $Cx43^{+/+}$ or $Cx43^{+/-}$ macrophages as compared with

cells infected with GFP alone (Fig. 4*C*, compare green bars to yellow bars). To further confirm the specificity of the effect of Cx43 on phagocytosis, $Cx43^{+/+}$, $Cx43^{+/-}$, and $Cx43^{-/-}$ macrophages were infected with adenoviruses that express a dominant-negative L90V mutation in the polypeptide backbone of Cx43 ([21]). Importantly, there was no increase in the rate of phagocytosis by embryonic hepatic macrophages obtained from $Cx43^{-/-}$ mice after infection with L90V-GFP Cx43 (see Fig. 4*C*, compare blue bars to yellow bars). It is noteworthy that the dominant-negative Cx43 construct significantly inhibited phagocytosis by $Cx43^{+/+}$ macrophages as expected (Fig. 4*C*, compare blue bars to green bars). Taken together, these findings demonstrate that Cx43 plays a role in macrophage phagocytosis.

Cx43 plays a role in the FcR-induced activation of RhoA and actin cup formation

We next sought to explore the mechanisms by which Cx43 could regulate phagocytosis in macrophages. To do so, we focused on the early signaling events that lead to particle internalization, which we and others have shown to require the activation of the Rho-GTPase family of small molecular mass G proteins ([18], [30], [31]). As shown in Fig. 5*A*, the activation of RhoA using LPA leads to an increase in phagocytosis, while inhibition of RhoA using the inhibitor Y27632 reduces phagocytosis. These findings replicate previous work confirming a role for RhoA in phagocytosis ([18], [32]). Strikingly, the inhibition of Cx43 in macrophages with Cx43 siRNA significantly reduced the extent of RhoA activation in RAW264.7 macrophages that was induced upon binding of IgG-opsonized particles (Fig. 5*B*), while the marked inhibition of phagocytosis that we previously observed in response to Cx43 inhibition could be reversed upon transfection of cells with constitutively active RhoA-GTP (Fig. 5*C*). This finding indicates RhoA activity could reverse the inhibition in phagocytosis that occurred in response to Cx43 inhibition, and it supports the notion that Cx43 activation may be linked to phagocytosis via RhoA signaling. Given that RhoA signaling leads to the formation of actin cups at the site of adherent particles ([18]), we next considered whether Cx43 may be required for actin cup formation. As shown in Fig. 5*D*, inhibition of Cx43 in RAW264.7 macrophages with Cx43 siRNA significantly reduced the formation of actin “cups” after adherence of opsonized latex beads, as compared with both untreated cells and cells treated with control siRNA against no known targets (see representative images in Fig. 5, *E*–*J*). Taken together, these results indicate that Cx43 is likely to participate in phagocytosis in vitro in part through RhoA-mediated effects on the actin cytoskeleton.

Cx43 participates in host survival after bacterial peritonitis

Having shown a role for the regulation of phagocytosis by Cx43 in vitro, we next sought to assess whether Cx43 could regulate phagocytosis in vivo and, if so, whether such regulation would affect the host response to bacterial infection of the peritoneal cavity. As shown in Fig. 6, *A*–*C*, intraperitoneal treatment of mice with the gap junction inhibitor oleamide led to a profound reduction in the phagocytosis of fluorescent-labeled bacteria that had been injected into the peritoneal cavity compared with animals injected with vehicle alone or noninjected mice. The inhibition of phagocytosis that was measured in response to oleamide injection was further revealed by the dose-dependent reduction in the ability of peritoneal macrophages to internalize opsonized particles after being exposed to intraperitoneal oleamide (Fig. 6*D*). There was no effect on phagocytosis of vehicle alone. To investigate the

potential physiological relevance of the role of Cx43 on phagocytosis, a model of bacterial peritonitis was utilized. The intraperitoneal inoculation of *E. coli* of mice resulted in a mortality of ~50% after 48 h (Fig. 6*E*). A similar rate of mortality was seen after 48 h in mice injected with *E. coli* along with vehicle alone (Fig. 6*E*). However, co-injection of oleamide with *E. coli* resulted in a mortality rate of nearly 100% after 48 h (Fig. 6*E*). There was no effect on mortality of injection with vehicle alone or oleamide alone. Importantly, the rate of phagocytosis in vivo of Oregon Green-labeled bacteria that had been injected into the peritoneal cavity was significantly reduced in $Cx43^{+/-}$ mice (Fig. 6, *G* and *H*) as compared with wild-type littermates (Fig. 6, *F* and *H*).

To further assess the role of Cx43 in the regulation of the host response to infection, and to extend these pharmacologic findings, we further assessed the ability of $Cx43^{+/-}$ mice to respond to an intraperitoneal bacterial challenge. As shown in Fig. 7, the injection of *E. coli* into the peritoneal cavities of $Cx43^{+/-}$ mice led to a significant increase in mortality on each subsequent day after injection compared with wild-type counterparts. The Kaplan-Meier survival curves for wild-type and $Cx43^{+/-}$ mice that had been injected with intraperitoneal *E. coli* reveal that $Cx43^{+/-}$ mice had a significantly increased mortality, at $p = 7.45 \times 10^{-5}$. Taken together, these results indicate that Cx43 plays a role in the host response to bacterial infection in vivo, and that this regulation has an effect on host survival after bacterial infection.

Discussion

We now report the novel finding that the gap junction protein Cx43 plays a previously unrecognized role in the regulation of phagocytosis by macrophages. While we acknowledge that the inhibition of Cx43 resulted in only a partial (albeit significant) inhibition in phagocytosis, the fact that three different techniques to reduce Cx43 function (pharmacologic, siRNA, and Cx43-mutant mice) yielded a similar reduction in phagocytosis, as well as the fact that a role for Cx43 in phagocytosis was observed in both cultured and primary macrophages, strongly argues that Cx43 plays at least a partial role in the complex process of phagocytosis. In seeking to understand the potential mechanisms involved, we further report that inhibition of Cx43 leads to an inhibition of FcR-induced activation of RhoA and a subsequent reduction in the extent of actin cup formation around adherent particles. Taken together, these findings expand on the known roles of Cx43 in immune cells such as macrophages, and they provide added insights into the signaling pathways that are required for particle internalization to occur.

How do we explain the involvement of Cx43 in phagocytosis? Given that macrophages exist as single cells, it is unlikely that Cx43 is exerting its role as a gap junction protein. However, Cx43 is a known component of hemichannels, the non-opposed halves of gap junction channels that are localized at the cell surface and intracellularly and function independently of gap junctions. It is possible that Cx43 could participate in the regulation of phagocytosis by acting via hemichannels on calcium regulation for instance, which is a known function of hemichannels ([33]) and is also known to play a role in phagocytosis ([34]). In support of this possibility, treatment of macrophages with oleamide, which is known to inhibit the function of hemichannels ([35], [36]), was found to inhibit phagocytosis. Alternatively, Cx43 may exert

other roles independent of hemichannel activity in macrophages that could regulate phagocytosis. Specifically, Cx43 has been shown to bind to a variety of actin regulatory proteins that could regulate actin cup formation and initiate phagocytosis ([10], [11], [37], [38]). Cx43 has been shown to participate in RhoA signaling cascade in astrocytes ([39]) and to interact with PSD95/Dlg/ZO-1 (PDZ) domains of various proteins ([40]), protein-protein binding regions that act to assemble membrane receptors and cytosolic proteins ([41]). PDZ domains have been found on proteins with established roles in the initiation of phagocytosis including the adaptor protein GIPC, a PDZ domain-containing protein, shown to regulate cytoskeletal dynamics ([42]). This suggests the possibility that Cx43 could act through its PDZ domain-binding region through similar regulatory targets in the initiation of phagocytosis. In support of the fact that Cx43 may interact with other proteins that are required for phagocytosis to occur, we note that that infection of macrophages with a L90V mutation in the polypeptide backbone of Cx43 resulted in a marked inhibition of phagocytosis in wild-type cells and did not reverse the inhibition of Cx43 observed in cells obtained from Cx43-deficient mice. This leads us to speculate that the L90V mutation in Cx43 renders Cx43 incapable of forming the necessary protein-protein interactions that are required for phagocytosis to occur. We now submit that acting either via hemichannels or in a more expanded manner through the interaction with protein targets that play important roles in the rearrangements of the actin cytoskeleton, Cx43 participates in the process of phagocytosis.

One of the most striking findings of the present study is that the inhibition of Cx43 in vivo, using either pharmacologic or genetic approaches, led to a marked increase in mortality after bacterial peritoneal sepsis. Previous authors have provided a link between connexin activity and sepsis. For instance, Fernandez-Cobo et al. have shown that the dysfunction in cardiac contractility that has been observed to occur in septic patients may be mediated by a down-regulation of Cx43 in the heart, possibly via the release of TNF-α ([43]). Celes et al. recently described a loss of Cx43 expression in the heart in mice subjected to a cecal ligation and puncture model of sepsis, lending further support to this concept ([44]). De Maio et al. have shown that the release of LPS, which often accompanies sepsis, leads to a loss of gap junction-mediated communication between hepatocytes, suggesting a possible role in the disordered hepatic metabolic function that occurs during inflammatory states ([45]), while the administration of LPS to monolayers of cultured mouse microvascular endothelial cells was found to reduce cell-to-cell communication through phosphorylation of Cx43 by tyrosine kinase ([46]). We therefore now propose that in addition to its established roles in gap junction communication, Cx43 may exert a broader role in the regulation of the host immune response and the development of sepsis.

We readily acknowledge that in addition to a direct role of Cx43 on phagocytosis, there are additional possible routes by which Cx43 heterozygosity could worsen outcome from infection. For instance, Cx43 has been shown to exert a role in cell migration ([47]–[49]), and it could therefore lead to an impairment in the ability of neutrophils to migrate to sites of bacterial infection, and as a result impair microbial clearance and worsen outcome after peritoneal infectious challenge. Alternatively, Cx43 has been shown to play a role in generation of reactive oxygen species ([50]). Any impairment in reactive oxygen species generation in macrophages, either extracellularly or within the phagosome itself, could

reduce microbial killing and worsen outcome in Cx43 heterozygous mice. If Cx43 hemichannels play a role in ATP transport into the phagosome, Cx43 heterozygosity could theoretically also impair microbial killing by limiting the extent of phagosomal acidification by limiting the local availability of free ATP and thus impair the function of the vacuolar type H^+-ATPase that is the driving force leading to phagosomal acidification ([25]). Alternatively, decreased Cx43 function could lead to impaired T and B lymphocyte function, resulting in decreased cytokine generation and impaired generation of Abs, functions that have recently been shown to involve Cx43 activity ([51]). Hence, although the current studies strongly indicate a role for Cx43 in phagocytosis, we acknowledge the possibility that other Cx43-mediated effects could also be involved that could lead to a worse outcome from bacterial infection that we observed in the Cx43 heterozygous animals.

In summary, we now demonstrate that the gap junction protein Cx43 plays a role in the regulation of phagocytosis through a mechanism that involves the RhoA-mediated rearrangement of the actin cytoskeleton that is required for particle internalization to occur. These studies shed light not only on an unexpected role for Cx43, but also raise important insights into the complex molecular armamentarium required for normal host defense.

Acknowledgments

We thank Dr. Matthias M. Falk (Lehigh University, Bethlehem, PA) for GFP-tagged Cx43 cDNA, Dr. Allan D. Schreiber, (University of Pennsylvania School of Medicine, Philadelphia, PA) for Fc-cDNA, Dr. Dale Laird (The University of Western Ontario, London, Ontario, Canada) for provision of wild-type and mutant Cx43 constructs, Dr. Chuck Murry (University of Washington, Seattle, WA) for GFP adenoviruses, and Dr. Michael S. Kolodney (University of California at Los Angeles School of Medicine) for constitutively active (V-14) RhoA. We also acknowledge Dr. Janet Rossant and Dr. A. Flenniken (Samuel Lunenfeld Research Institute, Mount Sinai Hospital, Toronto, Ontario, Canada) for expertise and advice regarding the maintenance of a colony of $Cx43^{+/-}$ mice, and for the initial provision of animals (all animals used in the experiments described in the present manuscript were obtained through The Jackson Laboratory).

References

1. Desjardins M, Huber LA, Parton RG, Griffiths G. Biogenesis of phagolysosomes proceeds through a sequential series of interactions with the endocytic apparatus. J. Cell Biol. 1994; 124:677–688. [PubMed: 8120091]
2. Hackam DJ, Rotstein OD, Sjolin C, Schreiber AD, Trimble WS, Grinstein S. v-SNARE-dependent secretion is required for phagocytosis. Proc. Natl. Acad. Sci. USA. 1998; 95:11691–11696. [PubMed: 9751727]
3. Stuart LM, Ezekowitz RA. Phagocytosis and comparative innate immunity: learning on the fly. Nat. Rev. Immunol. 2008; 8:131–141. [PubMed: 18219310]
4. Laird D. Life cycle of connexins in health and disease. Biochem. J. 2006; 394:527–543. [PubMed: 16492141]
5. Evans W, De Vuyst E, Leybaert L. The gap junction cellular internet: connexin hemichannels enter the signalling limelight. Biochem. J. 2006; 397:1–14. [PubMed: 16761954]
6. Stout C, Goodenough D, Paul D. Connexins: functions without junctions. Curr. Opin. Cell Biol. 2004; 16:507–512. [PubMed: 15363800]
7. Vieira O, Botelho R, Grinstein S. Phagosome maturation: aging gracefully. Biochem. J. 2002; 15:689–704. [PubMed: 12061891]
8. Cotrina M, Lin J, Alves-Rodrigues A, Liu S, Li J, Azmi-Ghadimi H, Kang J, Naus C, Nedergaard M. Connexins regulate calcium signaling by controlling ATP release. Proc. Natl. Acad. Sci. USA. 1998; 95:15735–15740. [PubMed: 9861039]

9. Giepmans BN. Role of connexin43-interacting proteins at gap junctions. Adv. Cardiol. 2006; 42:41–56. [PubMed: 16646583]
10. Giepmans BN, Verlaan I, Hengeveld T, Janssen H, Calafat J, Falk MM, Moolenaar WH. Gap junction protein connexin-43 interacts directly with microtubules. Curr. Biol. 2001; 11:1364–1368. [PubMed: 11553331]
11. Giepmans BN, Moolenaar WH. The gap junction protein connexin43 interacts with the second PDZ domain of the zona occludens-1 protein. Curr. Biol. 1998; 8:931–934. [PubMed: 9707407]
12. Beyer EC, Steinberg TH. Evidence that the gap junction protein connexin-43 is the ATP-induced pore of mouse macrophages. J. Biol. Chem. 1991; 266:7971–7974. [PubMed: 1708769]
13. Eugenín EA, González HE, Sánchez HA, Brañes MC, Sáez JC. Inflammatory conditions induce gap junctional communication between rat Kupffer cells both in vivo and in vitro. Cell. Immunol. 2007; 247:103–110. [PubMed: 17900549]
14. Bermudez-Fajardo A, Ylihärsilä M, Evans WH, Newby AC, Oviedo-Orta E. $CD4^+$ T lymphocyte subsets express connexin 43 and establish gap junction channel communication with macrophages in vitro. J. Leukocyte Biol. 2007; 82:608–612. [PubMed: 17596336]
15. Greenberg SS, Xie J, Spitzer JJ, Wang JF, Lancaster J, Grisham MB, Powers DR, Giles TD. Nitro containing L-arginine analogs interfere with assays for nitrate and nitrite. Life Sci. 1995; 57:1949–1961. [PubMed: 7475944]
16. Ren S, Li M, Cai H, Hudgins S, Furth PA. A simplified method to prepare PCR template DNA for screening of transgenic and knockout mice. Contemp. Top. Lab. Anim. Sci. 2001; 40:27–30. [PubMed: 11300684]
17. Morris L, Crocker PR, Gordon S. Murine fetal liver macrophages bind developing erythroblasts by a divalent cation-dependent hemagglutinin. J. Cell Biol. 1988; 106:649–656. [PubMed: 2831233]
18. Hackam DJ, Rotstein OD, Schreiber A, Zhang W, Grinstein S. Rho is required for the initiation of calcium signaling and phagocytosis by Fcγ receptors in macrophages. J. Exp. Med. 1997; 186:955–966. [PubMed: 9294149]
19. Neal MD, Leaphart C, Levy R, Prince J, Billiar TR, Watkins S, Li J, Cetin S, Ford H, Schreiber A, Hackam DJ. Enterocyte TLR4 mediates phagocytosis and translocation of bacteria across the intestinal barrier. J. Immunol. 2006; 176:3070–3079. [PubMed: 16493066]
20. Hackam DJ, Rotstein OD, Bennett MK, Klip A, Grinstein S, Manolson MF. Characterization and subcellular localization of target membrane soluble NSF attachment protein receptors (t-SNAREs) in macrophages: syntaxins 2, 3, and 4 are present on phagosomal membranes. J. Immunol. 1996; 156:4377–4383. [PubMed: 8666810]
21. McLachlan E, Manias JL, Gong XQ, Lounsbury CS, Shao Q, Bernier SM, Bai D, Laird DW. Functional characterization of oculodentodigital dysplasia-associated Cx43 mutants. Cell Commun. Adhes. 2005; 12:279–292. [PubMed: 16531323]
22. Reinecke H, Minami E, Virag JI, Murry CE. Gene transfer of connexin43 into skeletal muscle. Hum. Gene Ther. 2004; 15:627–636. [PubMed: 15242523]
23. Fujisawa K, Madaule P, Ishizaki T, Watanabe G, Bito H, Saito Y, Hall A, Narumiya S. Different regions of Rho determine Rho-selective binding of different classes of Rho target molecules. J. Biol. Chem. 1998; 273:18943–18949. [PubMed: 9668072]
24. Cetin S, Ford HR, Sysko LR, Agarwal C, Wang J, Neal MD, Baty C, Apodaca G, Hackam DJ. Endotoxin inhibits intestinal epithelial restitution through activation of Rho-GTPase and increased focal adhesions. J. Biol. Chem. 2004; 279:24592–24600. [PubMed: 15169791]
25. Hackam DJ, Rotstein O, Zhang W, Demaurex N, Woodside M, Tsai O, Grinstein S. Regulation of phagosomal acidification: differential targeting of Na^+/H^+ exchangers, Na^+/K^+-ATPases, and vacuolar-type H^+ ATPases. J. Biol. Chem. 1997; 272:29810–29820. [PubMed: 9368053]
26. Guan X, Cravatt BF, Ehring GR, Hall JE, Boger DL, Lerner RA, Gilula NB. The sleep-inducing lipid oleamide deconvolutes gap junction communication and calcium wave transmission in glial cells. J. Cell Biol. 1997; 139:1785–1792. [PubMed: 9412472]
27. Li WE, Waldo K, Linask KL, Chen T, Wessels A, Parmacek MS, Kirby ML, Lo CW. An essential role for connexin43 gap junctions in mouse coronary artery development. Development. 2002; 129:2031–2042. [PubMed: 11934868]

28. Downey GP, Botelho RJ, Butler JR, Moltyaner Y, Chien P, Schreiber AD, Grinstein S. Phagosomal maturation, acidification, and inhibition of bacterial growth in nonphagocytic cells transfected with FcγRIIA receptors. J. Biol. Chem. 1999; 274:28436–28444. [PubMed: 10497205]
29. Reaume AG, de Sousa PA, Kulkarni S, Langille BL, Zhu D, Davies TC, Juneja SC, Kidder GM, Rossant J. Cardiac malformation in neonatal mice lacking connexin43. Science. 1995; 267:1831–1834. [PubMed: 7892609]
30. Ridley AJ, Allen WE, Peppelenbosch M, Jones GE. Rho family proteins and cell migration. Biochem. Soc. Symp. 1999; 65:111–123. [PubMed: 10320936]
31. Hall A. Rho GTPases and the actin cytoskeleton. Science. 1998; 279:509–514. [PubMed: 9438836]
32. Caron E, Hall A. Identification of two distinct mechanisms of phagocytosis controlled by different Rho GTPases. Science. 1998; 282:1717–1721. [PubMed: 9831565]
33. Tran Van Nhieu G, Clair C, Bruzzone R, Mesnil M, Sansonetti P, Combettes L. Connexin-dependent inter-cellular communication increases invasion and dissemination of Shigella in epithelial cells. Nat. Cell Biol. 2003; 5:720–726. [PubMed: 12844145]
34. Yeung T, Gilbert GE, Shi J, Silvius J, Kapus A, Grinstein S. Membrane phosphatidylserine regulates surface charge and protein localization. Science. 2008; 319:210–213. [PubMed: 18187657]
35. Berra-Romani R, Raqeeb A, Avelino-Cruz JE, Moccia F, Oldani A, Speroni F, Taglietti V, Tanzi F. Ca^{2+} signaling in injured in situ endothelium of rat aorta. Cell Calcium. 2008; 44:298–309. [PubMed: 18276005]
36. Quist AP, Rhee SK, Lin H, Lal R. Physiological role of gapjunctional hemichannels: extracellular calcium-dependent isosmotic volume regulation. J. Cell Biol. 2000; 148:1063–1074. [PubMed: 10704454]
37. Giepmans BN. Gap junctions and connexin-interacting proteins. Cardiovasc. Res. 2004; 62:233–245. [PubMed: 15094344]
38. Park DJ, Freitas TA, Wallick CJ, Guyette CV, Warn-Cramer BJ. Molecular dynamics and in vitro analysis of connexin43: a new 14-3-3 mode-1 interacting protein. Protein Sci. 2006; 15:2344–2355. [PubMed: 17008717]
39. Rouach N, Pebay A, Meme W, Cordier J, Ezan P, Etienne E, Giaume C, Tence M. S1P inhibits gap junctions in astrocytes: involvement of G and Rho GTPase/ROCK. Eur. J. Neurosci. 2006; 23:1453–1464. [PubMed: 16553609]
40. Singh D, Solan JL, Taffet SM, Javier R, Lampe PD. Connexin 43 interacts with zona occludens-1 and -2 proteins in a cell cycle stage-specific manner. J. Biol. Chem. 2005; 280:30416–30421. [PubMed: 15980428]
41. Fanning AS, Anderson JM. PDZ domains: fundamental building blocks in the organization of protein complexes at the plasma membrane. J. Clin. Invest. 1999; 103:767–772. [PubMed: 10079096]
42. Bohlson SS, Zhang M, Ortiz CE, Tenner AJ. CD93 interacts with the PDZ domain-containing adaptor protein GIPC: implications in the modulation of phagocytosis. J. Leukocyte Biol. 1995; 77:80–89. [PubMed: 15459234]
43. Fernandez-Cobo M, Gingalewski C, Drujan D, De Maio A. Down-regulation of connexin 43 gene expression in rat heart during inflammation: the role of tumour necrosis factor. Cytokine. 1999; 11:216–224. [PubMed: 10209069]
44. Celes MR, Torres-Dueñas D, Alves-Filho JC, Duarte DB, Cunha FQ, Rossi MA. Reduction of gap and adherens junction proteins and intercalated disc structural remodeling in the hearts of mice submitted to severe cecal ligation and puncture sepsis. Crit. Care Med. 2007; 35:2176–2185. [PubMed: 17855834]
45. De Maio A, Gingalewski C, Theodorakis NG, Clemens MG. Interruption of hepatic gap junctional communication in the rat during inflammation induced by bacterial lipopolysaccharide. Shock. 2000; 14:53–59. [PubMed: 10909894]
46. Lidington D, Tyml K, Ouellette Y. Lipopolysaccharide-induced reductions in cellular coupling correlate with tyrosine phosphorylation of connexin 43. J. Cell Physiol. 2002; 193:373–379. [PubMed: 12384989]

47. Leaphart CL, Qureshi F, Cetin S, Li J, Dubowski T, Batey C, Beer-Stolz D, Guo F, Murray SA, Hackam DJ. Interferon-γ inhibits intestinal restitution by preventing gap junction communication between enterocytes. Gastroenterology. 2007; 132:2395–2411. [PubMed: 17570214]

48. Leaphart CL, Dai S, Gribar SC, Richardson W, Ozolek J, Shi XH, Bruns JR, Branca M, Li J, Weisz OA. Interferon-γ inhibits enterocyte migration by reversibly displacing connexin43 from lipid rafts. Am. J. Physiol. 2008; 295:G559–G569.

49. Zahler S, Hoffmann A, Gloe T, Pohl U. Gap-junctional coupling between neutrophils and endothelial cells: a novel modulator of transendothelial migration. J. Leukocyte Biol. 2003; 73:118–126. [PubMed: 12525569]

50. Ruiz-Meana M, Rodríguez-Sinovas A, Cabestrero A, Boengler K, Heusch G, Garcia-Dorado D. Mitochondrial connexin43 as a new player in the pathophysiology of myocardial ischaemia-reperfusion injury. Cardiovasc. Res. 2008; 77:325–333. [PubMed: 18006437]

51. Oviedo-Orta E, Howard Evans W. Gap junctions and connexin-mediated communication in the immune system. Biochim. Biophys. Acta. 2004; 1662:102–112. [PubMed: 15033582]

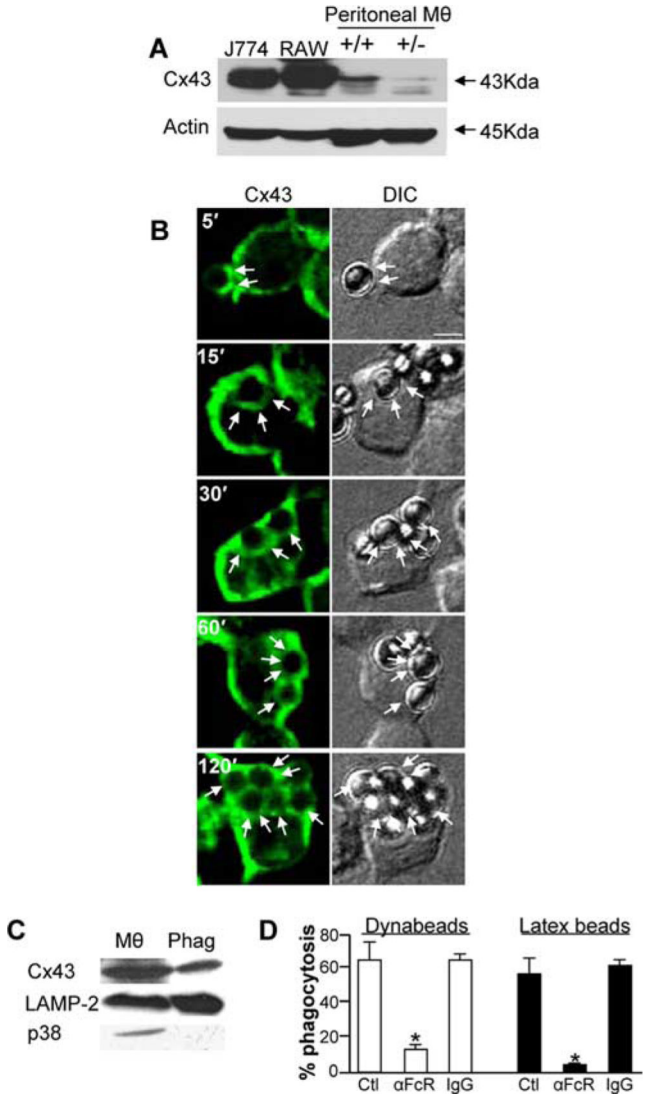

FIGURE 1.

Cx43 is expressed in macrophages and localizes to phagosomes. *A*, Macrophage cell lines, including J774 macrophages (J774), RAW 264.7 (RAW), and primary murine peritoneal macrophages (Mθ) from Cx43 wild-type (+/+) and heterozygous (+/−) mice, were subjected to SDS-PAGE and were assessed for the expression of Cx43 by immunoblotting. Blots were stripped and reprobed with Abs against F-actin. *B*, RAW264.7 macrophages were allowed to internalize Dynabeads for the indicated periods of time (5, 15, 30, 60, and 90 min) and then washed with copious amounts of PBS, fixed, permeabilized, and immunostained with Abs to Cx43 and imaged by confocal microscopy. Shown are the corresponding images for Cx43 (green) and DIC at each time point indicated. Arrows show the presence of bound (at 5 min) or internalized particles (at all other time points). Representative of three separate experiments. Size bar = 3 μm. *C*, Phagosomes (Phag) were isolated from J774 macrophages that had been fed a meal of latex beads and immunoblotted alongside J774 cells lysates (Mθ) using Abs against Cx43, LAMP-2, a phagosomal marker, and p38-MAPK (p38), a cytoplasmic protein expectedly absent from phagosomal membranes. Representative of three

separate experiments. *D*, Rate of phagocytosis after 1 h of either Dynabeads (open bars) or latex beads (filled bars) in RAW264.7 macrophages (open bars) or J774 cells (filled bars) that had been either untreated, treated with anti-FcR, or treated with nonspecific IgG.

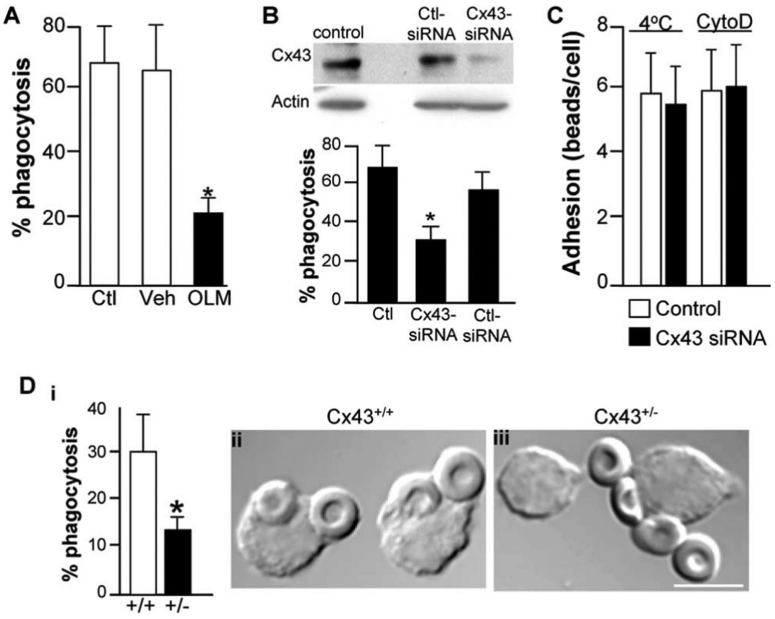

FIGURE 2.

Cx43 inhibition decreases phagocytosis by macrophages. *A*, J774 macrophages were either untreated (Ctl) or were treated with oleamide (OLM) or vehicle (Veh) and assessed for the ability to undergo phagocytosis of opsonized sheep erythrocytes. Representative of three separate experiments. *, $p < 0.05$. *B*, RAW264.7 macrophages were either untreated (control) or were treated with siRNA against either Cx43 (Cx43 siRNA) or against no known targets (Ctl siRNA). The expression of Cx43 and F-actin were assessed by Western blotting (*upper panel*). Shown is the quantification of phagocytosis. *, $p < 0.05$; representative of at least three separate experiments (*lower panel*). *C*, The adhesion of Dynabeads to RAW264.7 macrophages that were either treated with control siRNA (open bars) or with siRNA to Cx43 (filled bars). Adhesion occurred as shown either at 4°C or after treatment with the phagocytosis inhibitor cytochalasin D. *D*, The extent of phagocytosis of opsonized erythrocytes by peritoneal macrophages harvested from either wild-type (+/+) or Cx43 heterozygous mice (+/−). *, $p < 0.05$. Representative DIC micrographs of macrophages from wild-type (*ii*) and $Cx43^{+/-}$ mice (*iii*) that had been allowed to internalize SRBCs. Size bar = 5 μm.

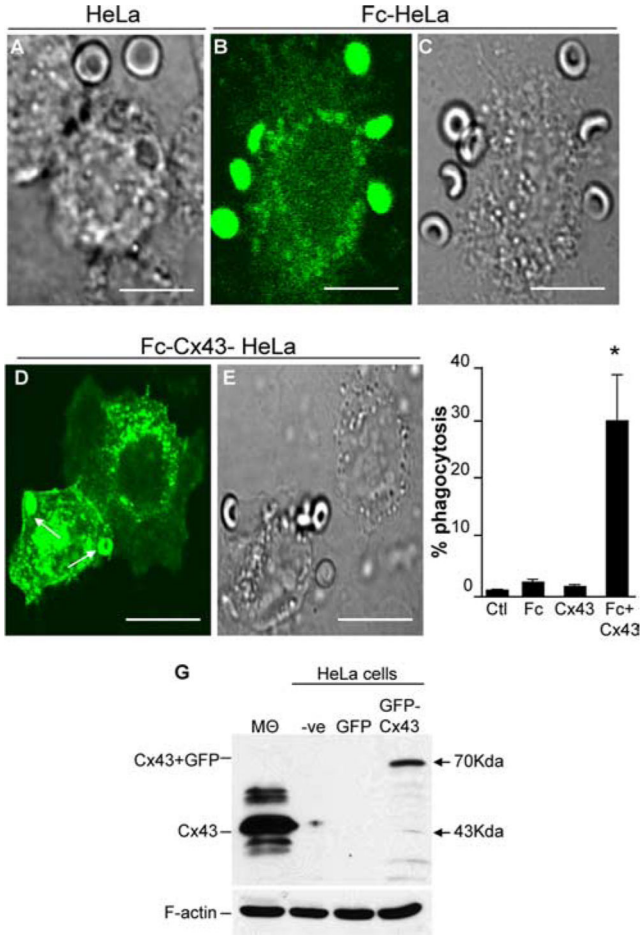

FIGURE 3.

Heterologous transfection of HeLa cells with Fc-Cx43 confers phagocytic ability. HeLa cells deficient in Cx43 were transfected with FcIIA and/or GFP and/or GFP-Cx43, then allowed to phagocytose SRBCs *A*, DIC micrograph of nontransfected HeLa cells in association with SRBCs (arrow). *B* and *C*, Confocal micrograph showing the GFP emission (*B*) and DIC image (*C*) revealing the distribution of SRBCs adherent to the surface of Fc-transfected HeLa cell. *D* and *E*, Confocal micrograph showing the GFP emission (*D*) and DIC image (*E*) of HeLa cells that had been cotransfected with FcRIIA and GFP-Cx43 and allowed to engulf SRBCs. Arrows show the presence of internalized SRBCs. Size bar = 10 μm. *F*, Phagocytosis capacity among the different groups. *, $p < 0.05$ vs control of at least seven separate experiments. *G*, SDS-PAGE with Abs to Cx43 in lysates obtained from RAW264.7 macrophages (Mθ, positive control), nontransfected HeLa cells (−ve), GFP-transfected HeLa cells (GFP), and GFP-Cx43-transfected HeLa cells (GFP-Cx43). Arrows show the location of Cx43 at 43 kDa in macrophages (the positive control) and GFP-Cx43 at 70 kDa in GFP-Cx43-transfected HeLa cells. Representative of three separate experiments.

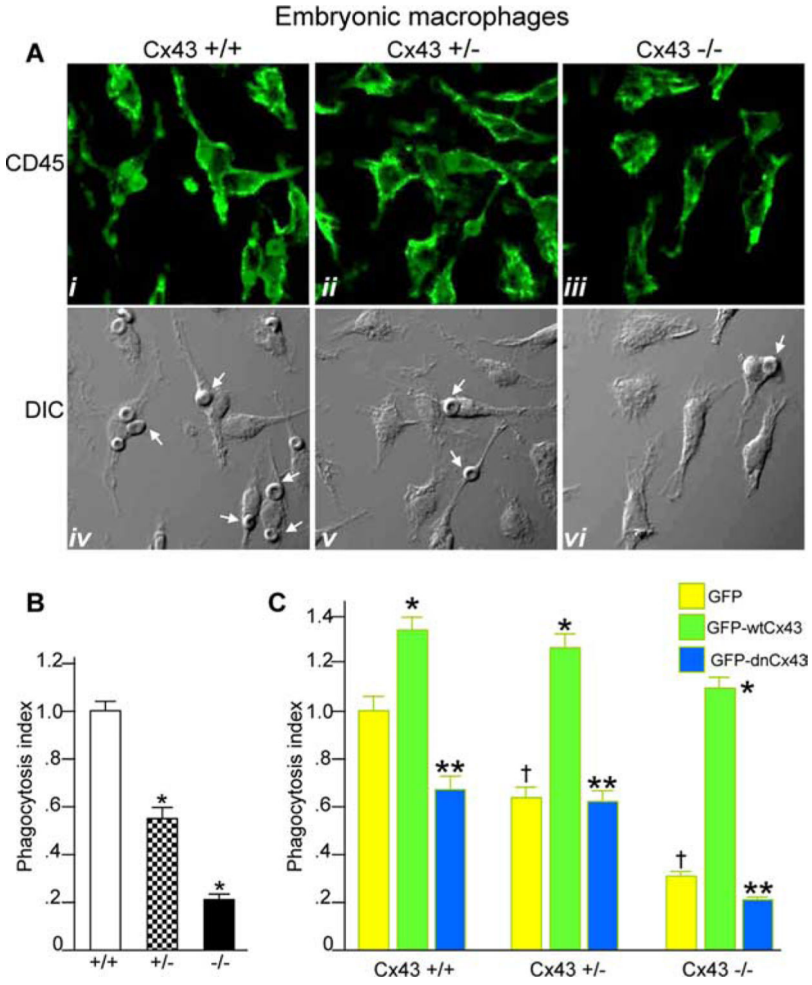

FIGURE 4.

Expression of adenovirus GFP-Cx43 reverses the impairment in phagocytosis observed in Cx43-deficient macrophages. *A*, Macrophages were harvested from the livers of embryonic $Cx43^{+/+}$, $Cx43^{+/-}$, and $Cx43^{-/-}$ mice at gestational age embryonic days 16–18 as described in *Materials and Methods*, immunostained with Abs against the macrophage marker CD45, and examined by confocal microscopy. Representative CD45 staining (*i-iii*) and the corresponding DIC images (*iv-vi*) are shown. *B*, Embryonic macrophages were harvested from livers of $Cx43^{+/+}$, $Cx43^{+/-}$, and $Cx43^{-/-}$ mice and allowed to internalize opsonized RBCs as described in *Materials and Methods*. The phagocytosis index (no. of cells with at least one internalized RBC per 100 cells relative to wild-type macrophages) is shown. Representative of five separate experiments. *, $p < 0.05$ vs wild-type macrophages. *C*, Macrophages were harvested from $Cx43^{+/+}$, $Cx43^{+/-}$, and $Cx43^{-/-}$ mice and infected with adenoviruses expressing GFP (yellow bars), GFP-wtCx43 (green bars), or GFP-dnCx43 (blue bars). Cells were then allowed to undergo phagocytosis of opsonized RBCs as described in *Materials and Methods*. The phagocytosis index (number of macrophages with at least one internalized particle per 100 cells relative to GFP-infected macrophages from each strain) is shown. †, $p < 0.05$ vs GFP-infected cells from wild-type mice. Note that in each case the rate of phagocytosis was decreased in GFP-infected cells from +/− and −/−

mice vs +/+ mice. *, $p < 0.05$ vs GFP-infected macrophages for each strain. Note that in each case infection with GFP-wtCx43 leads to a significant increase in phagocytosis; **, $p < 0.05$ vs GFP-wtCx43. Note that for each mouse strain, infection with GFP-dnCx43 leads to a significant decrease in the rate of phagocytosis compared with infection with wild-type Cx43. Representative of at least five separate experiments with more than five mice and 100 cells per group.

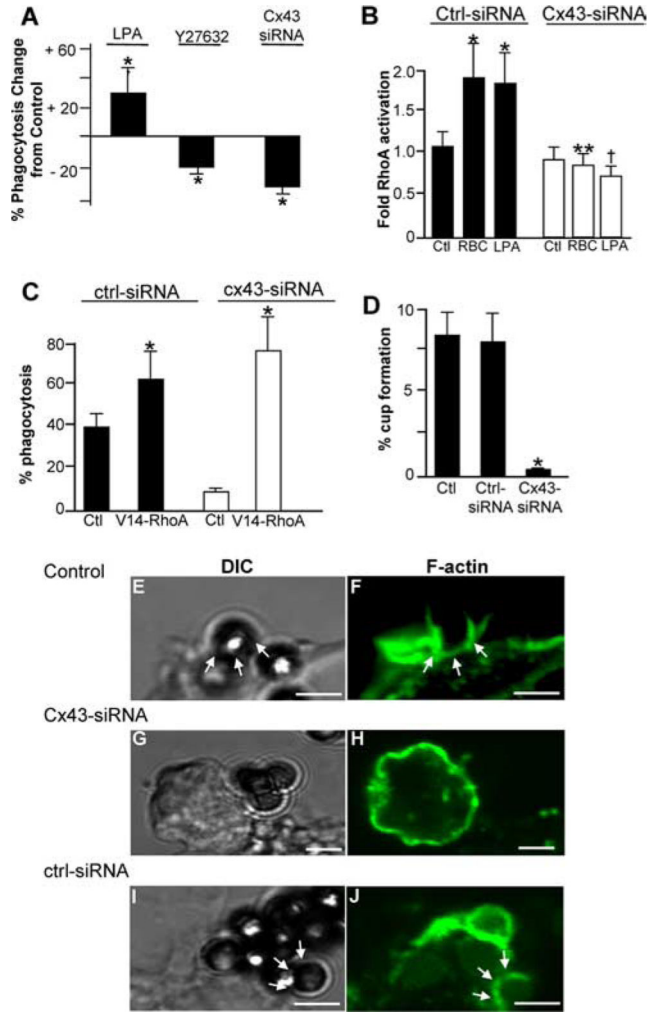

FIGURE 5.

Cx43 plays a role in the FcR-induced activation of RhoA and actin cup formation. *A*, J774 macrophages were treated with LPA (10 μM, a Rho activator), Y27632 (10 μM, a Rho inhibitor), or Cx43 siRNA, and assessed for the ability to internalize opsonized SRBCs, as compared with vehicle-treated control cells. *, $p < 0.05$; representative of at least five separate experiments. *B*, Fold activation of RhoA in RAW264.7 cells as assessed by ELISA after RAW264.7 cells had been transfected with either control siRNA or Cx43 siRNA, under the following conditions: untreated control (Ctl), IgG-opsonized SRBCs (RBC), or LPA (10 μM); *, $p < 0.05$ vs control; representative of at least five separate experiments; **, $p < 0.01$ vs control-siRNA RBC-treated cells; †, $p < 0.01$ vs control-siRNA LPA-treated cells. *C*, Phagocytosis capacity of RAW264.7 macrophages that had been treated with Cx43 siRNA or control siRNA then subsequently treated with media alone (Ctl) or transfected with constitutively active RhoA-GTP (V14-RhoA). *, $p < 0.05$ vs control for both control-siRNA or Cx43-siRNA; representative of at least three separate experiments. *D*, Percentage of macrophages shown to exhibit the formation of actin cups at the surface of RAW264.7 cells that had internalized IgG-opsonized RBCs, under the following conditions: untreated (Ctl), or transfected with control siRNA (Ctrl-siRNA) or siRNA to Cx43 (Cx43-siRNA). *E–J*,

Representative confocal micrographs showing actin cup formation around nascent SRBC phagosomes in RAW264.7 cells. Cells were either nontransfected (Control) or were transfected with the indicated siRNA. Size bar = 2 μm. Corresponding DIC images (*E*, *G*, and *I*) and F-actin fluorescence (*F*, *H*, and *J*) are displayed. Arrows indicate the formation of actin cups.

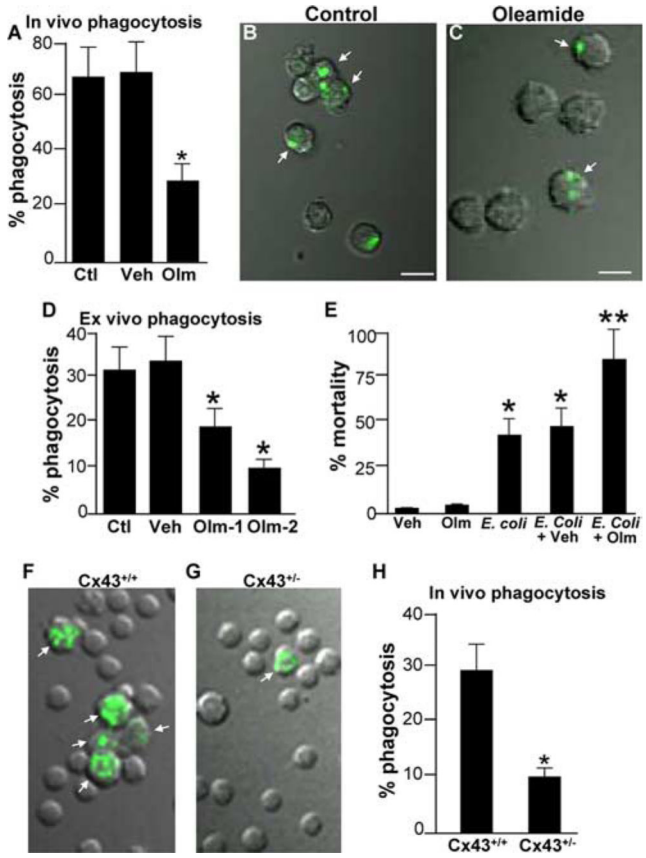

FIGURE 6.

Cx43 participates in phagocytosis in vivo and plays a role in host survival in response to bacterial peritonitis. *A*, Phagocytosis rate of Oregon Green-labeled *E. coli* by peritoneal macrophages of mice that had been injected i.p. either with saline (Ctl), vehicle (Veh), or oleamide (Olm, 25 mg/kg) daily for the preceding 3 days. *B* and *C*, Representative merged confocal images showing DIC (gray) and Oregon Green fluorescence (green staining) of macrophages obtained from mice that had been injected with either vehicle control (*B*) or oleamide (*C*). Arrows point to macrophages that had internalized bacteria. Representative of three separate experiments; $p < 0.05$. *D*, Rate of phagocytosis of IgG-opsonized SRBCs by peritoneal macrophages that had been harvested from mice that were injected i.p. with different concentrations of oleamide (Olm-1, 12.5 mg/kg; Olm-2, 25 mg/kg) or vehicle (Veh). *, $p < 0.05$, $n = 3$ separate experiments with three mice per experiment involving >100 macrophages per mouse. *E*, Percentage mortality 48 h after injection of mice with 8×10^8 CFU live *E. coli* in addition to either oleamide alone (Olm), vehicle alone (Veh), *E. coli* alone, *E. coli* plus vehicle (*E. coli* + Veh), or *E. coli* plus oleamide (50 mg/kg, *E. coli* + Olm). *, $p < 0.05$, representative of five separate experiments. *F–H*, Representative merged confocal images showing DIC (gray) and Oregon Green fluorescence (green staining) of macrophages obtained from wild-type mice (*F*) or $Cx43^{+/-}$ mice (*G*). Arrows point to macrophages that had internalized bacteria. Quantification is shown in *H*. Representative of three separate experiments; *, $p < 0.05$.

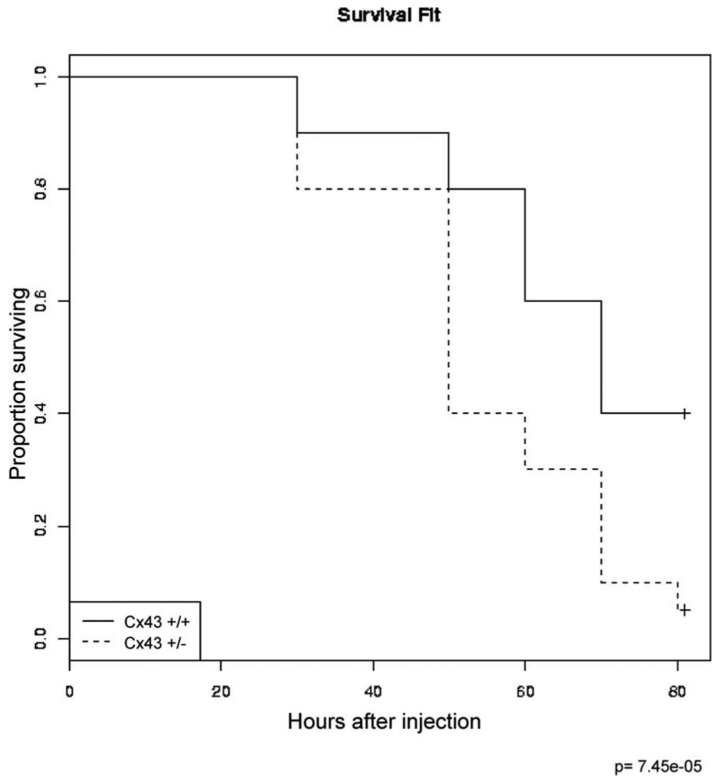

FIGURE 7.

Cx43-deficient mice demonstrate reduced survival after bacterial peritoneal sepsis. Age- and weight-matched $Cx43^{+/+}$ (solid lines) and $Cx43^{+/-}$ mice (dashed lines) ($n = 10$/group) were injected with *E. coli* daily for 3 days as described in *Materials and Methods*. Shown are Kaplan-Meier survival curves revealing the proportion of mice that are alive in each group as a function of time from the first injection of bacteria.